miR-103/107 promote ER stress-mediated apoptosis via targeting the Wnt3a/β-catenin/ATF6 pathway in preadipocytes

Zhenzhen Zhang, Song Wu, Saeed Muhammad, Qian Ren, and Chao Sun[1]

College of Animal Science and Technology, Northwest A&F University, Yangling, Shaanxi 712100, China

ORCID IDs: 0000-0002-4701-0252 (Z.Z.); 0000-0003-4824-1535 (S.W.); 0000-0001-5048-5753 (S.M.); 0000-0003-3305-8439 (Q.R.); 0000-0001-7222-4028 (C.S.)

Abstract Both miR-103 and miR-107 have been demonstrated to restrain cell proliferation and regulate lipid metabolism and inflammation. However, the effects of miR-103/107 on preadipocyte apoptosis remain unknown. In the present research, we have investigated how miR-103/107 regulated preadipocyte apoptosis. We found that miR-103/107 aggravated endoplasmic reticulum (ER) stress-mediated apoptosis in preadipocytes. We confirmed that miR-103/107 targeted WNT family member 3a (Wnt3a) in preadipocytes. It was found that overexpressing Wnt3a resulted in suppression of ER stress-mediated apoptosis, while restoration of miR-103/107 counteracted the effects of Wnt3a in preadipocytes. Moreover, bioinformatics and luciferase assays indicated that activating transcription factor (ATF)6 is a key player linking miR-103/107-induced ER stress to apoptosis. *ATF6* is regulated by lymphoid enhancer-binding factor 1, a transcription factor downstream of the Wnt3a/β-catenin signaling pathway, and ATF6 binds to the B-cell lymphoma 2 (*Bcl2*) promoter to regulate apoptosis further.**JLR** In conclusion, miR-103/107 promoted ER stress-mediated apoptosis by targeting the Wnt3a/β-catenin/ATF6 signaling pathway in preadipocytes. This study revealed that the miR-103/107-Wnt3a/β-catenin-ATF6 pathway is critical to the progression of apoptosis in preadipocytes, which suggested that approaches to activate miR-103/107 could potentially be useful as new therapies for treating obesity and metabolic syndrome-related disorders.—Zhang, Z., S. Wu, S. Muhammad, Q. Ren, and C. Sun. **miR-103/107 promote ER stress-mediated apoptosis via targeting the Wnt3a/β-catenin/ATF6 pathway in preadipocytes.** *J. Lipid Res.* 2018. **59:** 843–853.

Supplementary key words miR-103 and miR-107 • endoplasmic reticulum stress • WNT family member 3a/β-catenin-activating transcription factor 6 pathway

Currently, obesity is a global epidemic with morbidity increasing at a particularly high rate (1). Obesity, characterized by excessive adipose tissue, is related to some metabolic diseases, such as hypertension, cardiovascular disease, and type 2 diabetes mellitus (2, 3). As an important factor of obesity, adipose tissue has become a new target for obesity treatment. Except for adipogenesis and lipolysis, adipocyte death due to apoptosis has been demonstrated to play a very important role in the loss of adipose tissue. Adipose tissue contains a considerable amount of fibroblast-like preadipocytes. Preadipocytes have the ability to proliferate to produce new adipocytes and differentiate into mature adipocytes as well, which account for healthy adipose tissue turnover. Thus, induction of preadipocyte apoptosis may be an effective approach for obesity treatment.

microRNAs (miRNAs) are a class of small (∼18–25 nt) single-stranded noncoding RNAs, which function as endogenous regulators by targeting mRNAs (4). miRNA dysfunction is related to a variety of human diseases, such as obesity and metabolic disorders, suggesting that miRNAs play a promising role in obesity (5, 6). Aberrant expression of miRNAs, including miR-221, miR-519d, miR-141, and miR-520e, is associated with human obesity and related metabolic syndrome (7–9). miR-103 and -107 belong to the same family, differing only at one nucleotide residue close to their 3′ ends. It has been documented that miR-103/107 can retard tumor angiogenesis, promote adipogenesis, suppress cell proliferation, regulate lipid metabolism, and control insulin sensitivity (10–12). However, to date, the

roles of miR-103 and miR-107 in preadipocyte apoptosis have remained unknown.

The Wnt signaling pathway plays a pivotal role in embryonic development and apoptosis regulation. Studies have shown that the canonical Wnt/β-catenin pathway participates in multiple biological functions, including apoptosis and proliferation, by targeting downstream genes (13). WNT family member 3a (Wnt3a) is a canonical Wnt ligand that is an important regulator of various developmental processes, especially osteogenesis, apoptosis, adipogenesis, and mitochondrial biogenesis (14). Wnt ligands, including Wnt3a, bind to the cell surface Frizzled receptor family and regulate β-catenin stabilization and translocation to the nucleus where they can interact with the DNA-bound T cell factor/lymphoid enhancer factor (TCF/LEF) family to regulate the transcription of target genes (15, 16). In the absence of Wnts, β-catenin in cytoplasm is constantly degraded by the degradation compounds, which prevents β-catenin from reaching the nucleus, resulting in target genes being restricted by the TCF/LEF family (17).

The endoplasmic reticulum (ER) is an important organelle in cells. It is not only the place for protein folding and transportation, but is also important for intracellular Ca^{2+} storage and the synthesis of cholesterol, steroids, and many lipids (18, 19). A variety of physiological or pathological conditions, such as inhibition of protein glycosylation and imbalance of calcium homeostasis, will cause unfolded or misfolded protein in the ER to accumulate and, thus, damage normal ER physiological function (termed ER stress) (20, 21). Under these conditions, the ER activates the unfolded protein response to pause early protein synthesis and reduce the unfolded or misfolded protein in the ER, thus restoring normal physiological function and protecting cells. However, if the ER stress continues or cannot be alleviated, the signal will ultimately cause apoptosis (22, 23).

In the present study, we treated preadipocytes with palmitate or serum-free medium and found that miR-103 and -107 levels increased sharply. Bioinformatics analysis and dual-luciferase reporter assays revealed that Wnt3a, which is involved in processes related to adipocytes, is a novel target of miR-103/107. miR-103/107 promoted ER stress-mediated apoptosis and Wnt3a decreased ER stress-mediated apoptosis. Furthermore, miR-103/107 were found to inhibit the canonical Wnt/β-catenin signaling pathway, with lymphoid enhancer-binding factor 1 (LEF1)/activating transcription factor (ATF)6/B-cell lymphoma 2 (Bcl2) transcription playing a critical role in miR-103/107 aggravated ER stress-mediated apoptosis. Considering these results, it could be concluded that miR-103/107 played an important role in facilitating ER stress-mediated apoptosis in preadipocytes by targeting Wnt3a.

MATERIALS AND METHODS

Primary preadipocyte culture

The preparation of primary preadipocyte culture was as described before (24). Briefly, the eWAT tissues were washed three times with PBS buffer containing 200 U/ml penicillin (Sigma, St. Louis, MO) and 200 U/ml streptomycin (Sigma). The connective fiber and blood vessels were removed, and then preadipocytes were seeded onto culture dishes at 30% confluency and incubated at 37°C under a humidified atmosphere of 5% CO_2 and 95% air until confluence.

Differentiation of preadipocytes was performed as follows (25). Cells grown to 100% confluence (day 0) were induced to differentiate using DMEM/F12 medium containing dexamethasone (1 μM; Sigma), insulin (10 μg/ml; Sigma), IBMX (0.5 mM; Sigma), and 10% FBS. Four days after the induction (from day 2), cells were maintained in the induction medium containing insulin (10 μg/ml; Sigma) and 10% FBS.

Cell stimulation

The miR-103 and -107 mimics, inhibitor, miRNA negative control, siATF6, and siBcl2 were purchased from Gemma (Shanghai, China). Wnt3a and ATF6 CDS were cloned into pc-DNA 3.1(+) to generate plasmid vector. Preadipocytes were transfected at 70% confluence using X-tremeGENE HP DNA transfection reagent (Roche, Carlsbad, CA). The transfection procedure followed the protocol provided by the manufacturer.

For stimulation, preadipocytes were treated with 250 nM palmitate (Sigma) for 24 h. The 4-phenylbutyric acid (4-PBA) (50 μM) (Selleck, Shanghai, China) was incubated for 2 h to relieve ER stress. Dickkopf1 (DKK1) (150 ng/ml) (Selleck) was incubated for 3 h to block the canonical Wnt pathway.

RNA extraction and cDNA synthesis

Total RNA, including miRNA, was extracted from cells using TRIzol reagent (Invitrogen Life Technologies, Carlsbad, CA). cDNA was synthesized using a PrimeScript™ II First Strand cDNA RT synthesis kit (Takara Biotechnology Co., Ltd., Dalian, China). The mature miRNA was additionally reverse transcribed with the miRNA-specific stem-loop primer (5′ GAAAGAAGGCGAGGAGC-AGATCGAGGAAGAAGACGGAAGAATGTGCGTCTCGCCTTC-TTTCNNNNN 3′).

Quantitative PCR analysis

Quantitative (q)PCR was used to detect the relative mRNA expression levels with AceQ qPCR SYBR Green Master Mix (Vazyme), as described in Gan et al. (26). GAPDH and U6 were used to normalize mRNA and miRNA levels, respectively. The relative gene expressions were calculated using the $2^{-\Delta\Delta Ct}$ method. Primer sequences were as follows: miR-103-F, AGCAGCATTGTACAGGGC-TATGA; miR-107-F, AGCAGCATTGTACAGGGCTATCA; miRNA-R, AAGGCGAGACGCACATTCTT; U6-F, CTCGCTTCGGCAGCACA; U6-R, AACGCTTCACGAATTTGCGT; Wnt3a-F, ATGCCTCAGAGA-TGTTGCCTCACT; Wnt3a-R, TCAGATGGGTCCTGAAACAACCCT; Bcl2-associated X protein (Bax)-F, CAGGATGCGTCCACCAA; Bax-R, AAAGTAGAAGAGGGCAACCAC; Bcl2-associated death protein (Bad)-F, TGAGCCGAGTGAGCAGGAA; Bad-R, GCCTC-CATGATGACTGTTGGT; Bcl2-interacting mediator of cell death (Bim)-F, GACAGAACCGCAAGGTAATCC; Bim-R, ACTTGTCA-CAACTCATGGGTG; Bcl2-F, GGGAGAACAGGGTACGATAA; Bcl2-R, TACCCAGCCTCCGTTATCC; glucose-regulated protein 78 (Grp78)-F, GCATCACGCCGTCGTATGT; Grp78-R, ATTC-CAAGTGCGTCCGATGAG; CCAAT/enhancer-binding protein-homologous protein (Chop)-F, CTCGCTCTCCAGATTCCAGTC; Chop-R, CTTCATGCGTTGCTTCCCA; Atf4-F, CCTGAACAGC-GAAGTGTTGG; Atf4-R, TGGAGAACCCATGAGGTTTCAA; Atf6-F, TCGCCTTTTAGTCCGGTTCTT; Atf6-R, GGCTCCATAG-GTCTGACTCC; GAPDH-F, AATGGATTTGGACGCATTGGT; GAPDH-R, TTTGCACTGGTACGTGTTGAT.

miRNA target gene prediction

To predict the miRNA target gene, we used the following software: TargetScan (http://www.targetscan.org/vert_71/), miR-Base (http://www.mirbase.org/), and PicTar (http://www.pictar.org/). In order to improve the accuracy of the forecast, we chose their intersection to carry out our research.

Reporter constructs and dual-luciferase reporter assays

The dual-luciferase reporter assay procedure was performed as described in Liu et al. (27). The fragment of the 3′-untranslated region (UTR) of *Wnt3a* for miR-103 and miR-107 was synthesized and cloned into the region of the PGL3 vector. The mutant of the Wnt3a vector (PGL3-Wnt3a–mut) was cloned the same way.

For the luciferase assay, the renal luciferase expression plasmid (pRL-TK) vector and the pGL3 vector containing the wild-type fragment of the 3′-UTR of Wnt3a or a mutation fragment were transfected into 293T cells with miR-103 mimics or control. Forty-eight hours later, cells were harvested to analyze the luciferase activity using the Dual Luciferase Reporter Assay kit (Promega, Madison, WI).

Caspase-3 activity measurement

Caspase-3 activities were determined using a Caspase-Glo® 3 assay system (Promega) according to the manufacturer's instructions.

Apoptosis analysis by flow cytometry

Preadipocytes were transfected with miR-103/107 mimics, inhibitor, or control prior to apoptosis assessment. The Annexin V-FITC apoptosis detection kit (Vazyme, Nanjing, China) was used to analyze cell apoptosis. The procedure followed the protocol provided by the manufacturer. The data were analyzed with FCS Express software.

TUNEL staining

The TUNEL BrightGreen apoptosis detection kit (Vazyme) was further used to detect apoptosis. The procedure followed the protocol provided by the manufacturer.

Western blot

Western blot analysis was performed using standard methods as described in Gan et al. (28). The primary antibodies used were anti-Wnt3a (Abcam, ab28472), anti-Bax (Abcam, ab32503), anti-Bcl2 (Bioworld, bs1511), anti-GRP78 (Abcam, ab108615), anti-CHOP (Abcam, ab179823), anti-caspase-3 (Bioworld, bs6428), anti-active caspase-3 (Bioworld, bs7004), anti-β-actin (Bioworld, ap0060), and anti-GAPDH (Bioworld, ap0063). The rabbit secondary antibody was purchased from Abcam.

Nuclear protein extraction

The nuclear fractions were prepared as described in Liu et al (25). Briefly, cells were lysed with cytoplasmic lysis buffer. The lysates were centrifuged and supernatants were collected as cytoplasmic fractions. The pellets were resuspended in nuclear extraction buffer. Then the nuclear fractions were centrifuged and the supernatant was collected to obtain nuclear proteins. The proteins were denatured by boiling and kept for further studies.

Immunofluorescent staining

Immunofluorescent staining was performed as described (25). After being fixed with 4% paraformaldehyde and blocked with 5% BSA, the cells were incubated with rabbit polyclonal primary antibody overnight, followed by incubation with fluorescein isothiocyanate-conjugated goat anti-rabbit IgG antibody (Boster, Wuhan, China). DAPI was used for nuclear staining. Finally, cells were observed and photographed using a fluorescence microscope.

Data analysis

All experiments were repeated at least three times. The data are expressed as mean ± SD. The statistical analysis of differences was performed in GraphPad Prism 5.0 using *t*-test. $P < 0.05$ (*) was considered to show statistical significance and $P < 0.01$ (**) means very significant.

RESULTS

Wnt3a is a target gene of miR-103/107

In order to understand the biological functions of miR-103/107, we used three different programs to identify the potential molecular targets of miR-103/107. For miRNAs known to regulate target mRNAs by binding to their 3′-UTR regions, Wnt3a was identified as a potential target of miR-103/107 based on sequences in its 3′-UTR region that were complementary to the seed sequences of miR-103/107. Moreover, we found that these sequences of *Wnt3a* were evolutionarily conserved (**Fig. 1A**). Dual-luciferase reporter assays were performed to determine whether miR-103/107 directly targets Wnt3a. Cotransfection of miR-103 or -107 mimics with a wt-Wnt3a-3′-UTR luciferase reporter vector resulted in about a 28% decline of luciferase activity than that in the transfection with mutation groups (Fig. 1B). Furthermore, Western blot analysis indicated that overexpression of miR-103/107 by transfection miR-103 or miR-107 mimics decreased Wnt3a expression by 25% and 12%, respectively, compared to the control, while inhibition of miR-103 or -107 by transfection miR-103/107 inhibitor resulted in an approximately 35% increase of Wnt3a levels (Fig. 1C). In addition, we also detected the mRNA levels of miR-103/107 and *Wnt3a* during the process of adipocyte differentiation, finding that miR-103/107 and *Wnt3a* had opposite trends (Fig. 1D). In summary, these results clearly suggested that miR-103/107 directly target and suppress Wnt3a.

miR-103/107 were upregulated in preadipocytes on treatment with palmitate and serum-free medium

Two different types of apoptosis model were used to investigate the roles of miR-103/107 in preadipocyte apoptosis. We found that mRNA levels of *Bcl-2-associated X protein (Bax)* were increased by about 78% and 191%, while *Bcl2* mRNA experienced a degradation of 43% and 56% after 24 h incubation with serum-free medium and 250 nM palmitate, respectively, meaning a 24 h incubation period was sufficient to induce apoptosis. (**Fig. 2A**, F). Furthermore, Western blot results also indicated that serum-free medium caused a 50% increase of Bax and an 18% decrease of Bcl2 (Fig. 2B), and 250 nM of palmitate resulted in a 53% increase of Bax and a 55% decrease of Bcl2 (Fig. 2G). We also examined levels of miR-103/107 and *Wnt3a* in these models over several time points and found that palmitate and serum starvation treatment induced increases of about 150% and 110% expression of miR-103/107, respectively, while expression of *Wnt3a* was downregulated significantly (Fig. 2C, H). Reports have indicated that continuous ER stress ultimately leads to
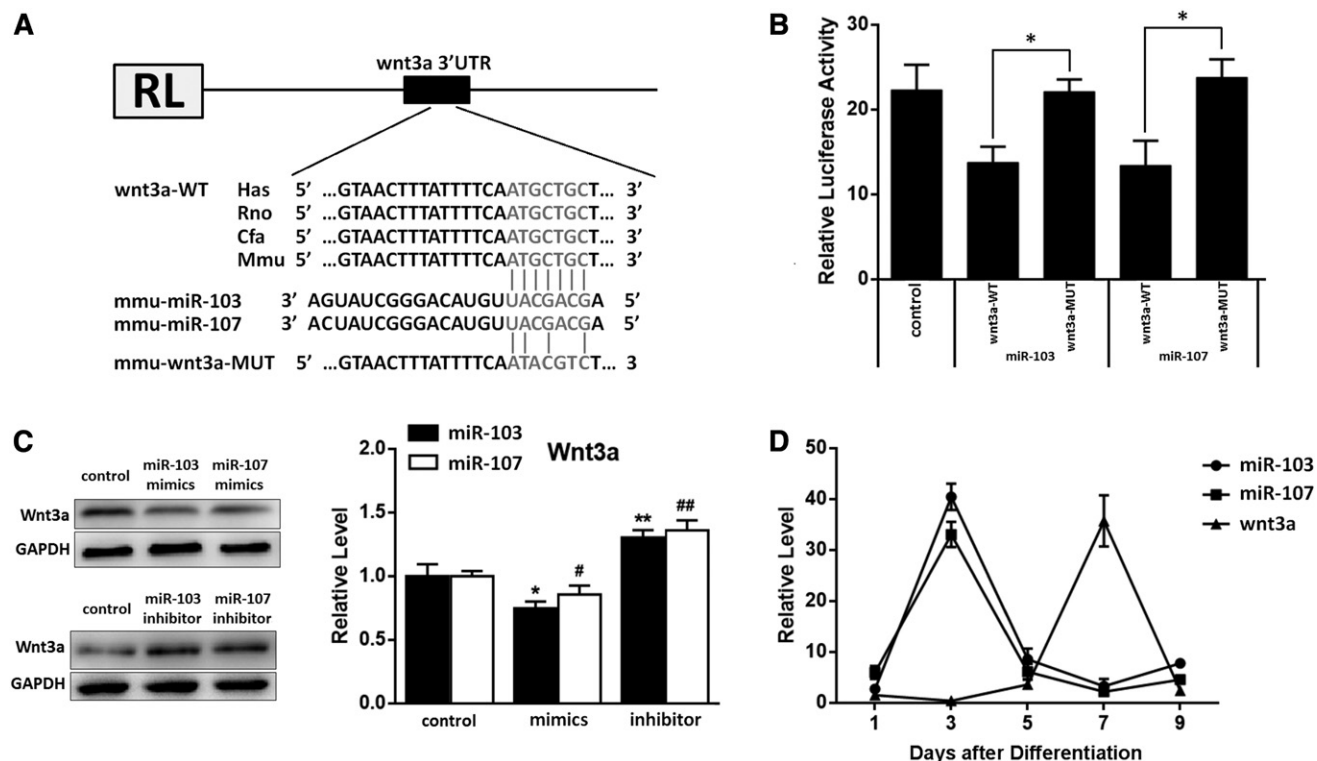
Fig. 1. Wnt3a is a target gene of miR-103/107. A: Scheme of the potential binding sites of miR-103/107 in the Wnt3a 3′-UTR. B: Double-luciferase assay was performed in 293T cells 48 h after miR-103/107 mimics transfected with Wnt3a-wt 3′-UTR or Wnt3a-mut 3′-UTR. C: Changes of Wnt3a protein level after 48 h transfected with miR-103/107 mimics, inhibitors, or control. D: Changes of miR-103/107 and *Wnt3a* mRNA levels in the process of adipocyte differentiation. Data represent the mean ± SD (* or [#]$P < 0.05$; ** or [##] $P < 0.01$. n ≥ 3).

apoptosis, so we decided to probe the role of ER stress in this process. The levels of ER stress factors, GRP78 and CHOP, were detected to evaluate the ER stress level. After 24 h of serum-free medium treatment, GRP78 was found to increase by 97% and 75% at mRNA and protein level, respectively, and CHOP was found to elevate to 312% and 141% at mRNA and protein level, respectively (Fig. 2D, E). Palmitate (250 nM) incubation resulted in *GRP78* and *CHOP* mRNA being increased to 297% and 206%, respectively (Fig. 2I). The protein levels of GRP78 and CHOP were found to elevate by 31% and 37%, respectively (Fig. 2J). These results indicated that both serum starvation and palmitate treatment activate ER stress, and miR-103/107 may play important roles in serum starvation- and palmitate treatment-activated ER stress and apoptosis.

miR-103/107 mimics promoted preadipocyte ER stress and apoptosis

Based on this data and previous literature reports, 250 nM of palmitate was chosen as an apoptotic model to elucidate the roles of miR-103/107 in preadipocyte ER stress and apoptosis. In this study, preadipocytes were transfected with miR-103/107 mimics or miRNA mimics as a negative control. ER stress and apoptotic markers were determined by qPCR and Western blot. As displayed in **Fig. 3A**, miR-103/107 mimics effectively enhanced miR-103 or -107 level, respectively. We found that miR-103/107 mimics dramatically increased the mRNA levels of *GRP78*, *CHOP*,

ATF4, and *ATF6* (Fig. 3B), and the protein levels of GRP78 and CHOP were also upregulated significantly (Fig. 3C), indicating that miR-103/107 activated ER stress. It was also found that the mRNA levels of *Bad*, *Bim*, and *Bax* were increased, while the *Bcl2* mRNA level was decreased to about 55% compared to the control (Fig. 3D). Interestingly, except for the upregulated Bax and downregulated Bcl2 protein levels, we also observed that the expression of active caspase-3 was elevated by 10–30% (Fig. 3E). So we examined caspase-3 activity and found that caspase-3 activity was raised to 1.82 ± 0.18, 1.60 ± 0.30, and 1.62 ± 0.16 after miR-103, miR-107, or both, respectively (Fig. 3G). Moreover, with TUNEL staining, we found that miR-103/107 mimics increased positive cell number (Fig. 3F). After Annexin V-FITC/PI staining, flow cytometry analysis also showed that treatment with miR-103/107 mimics increased the proportion of apoptotic cells from 52.94 ± 2.13% to 66.61 ± 3.25% and from 64.90 ± 4.06% to 62.85 ± 2.78%, respectively (Fig. 3H).

miR-103/107 knockdown suppressed ER stress and apoptosis in preadipocytes

To confirm the roles of miR-103/107 on preadipocyte ER stress and apoptosis, we carried out studies using a miR-103/107 inhibitor to knockdown miR-103/107 (**Fig. 4A**). As expected, miR-103/107 inhibitor downregulated the mRNA levels of *GRP78*, *CHOP*, *ATF4*, and *ATF6* (Fig. 4B). Western blot analysis revealed that GRP78 experienced a degradation of approximately 30–40% after miR-103/107
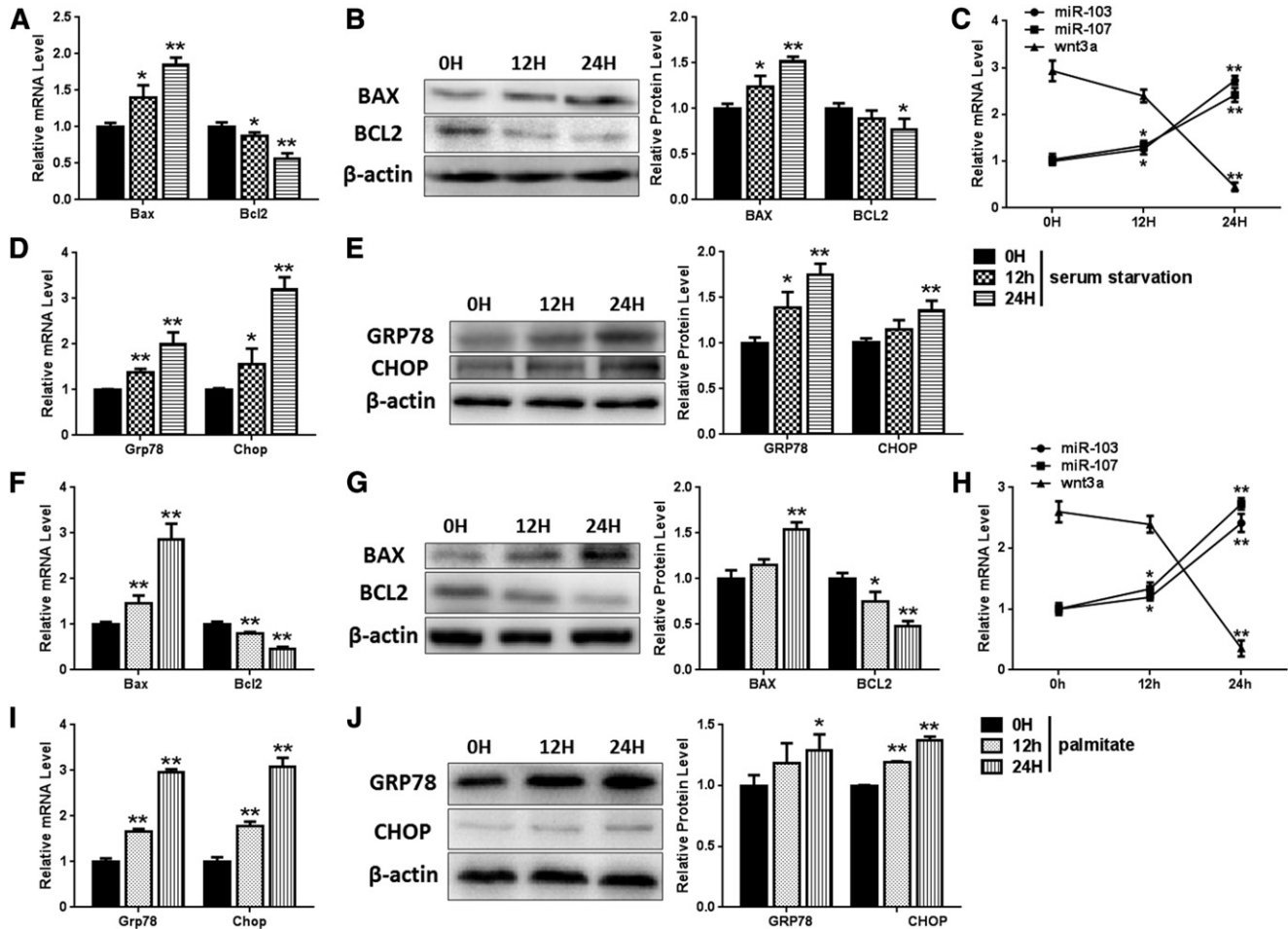
Fig. 2. miR-103/107 were upregulated in apoptosis models. Preadipocytes were treated with serum-free medium (A–E). A: The mRNA levels of *Bax* and *Bcl2*. B: The protein levels of Bax and Bcl2. C: Changes of miR-103/107 and *Wnt3a* mRNA levels. D: The mRNA levels of *GRP78* and *CHOP*. E: The protein levels of GRP78 and CHOP. Preadipocytes were treated with palmitate (F–J). F: The mRNA levels of *Bax* and *Bcl2*. G: The protein levels of Bax and Bcl2. H: The changes of miR-103/107 and *Wnt3a* mRNA levels. I: The mRNA levels of *GRP78* and *CHOP*. J: The protein levels of GRP78 and CHOP. Data represent the mean ± SD (*$P < 0.05$; **$P < 0.01$; n ⩾ 3).

inhibitor transfection, and CHOP had the same change (Fig. 4C). In addition, the mRNA levels of *Bad, Bim,* and *Bax* were also reduced significantly, while the level of *Bcl2* mRNA was raised to 150–170% in miR-103/107 inhibitor groups compared with the miRNA inhibitor negative control group (Fig. 4D).Western blot analysis revealed that miR-103/107 inhibitor decreased the protein levels of Bax and active caspase-3, as well as upregulated the expression of Bcl2 (Fig. 4E). Caspase-3 activity was found to be reduced by 40–60% after miR-103/107 inhibitor treatment (Fig. 4G). Furthermore, TUNEL staining and flow cytometry analysis revealed that suppressing miR-103/107 decreased the number of apoptotic cells compared with the control (Fig. 4F, H). Therefore, these findings suggested that miR-103/107 promoted ER apoptosis in preadipocytes as well.

Wnt3a relieved the effects of miR-103/107 on preadipocyte ER stress and apoptosis

Because we had shown that miR-103 and -107 directly targeted Wnt3a, we carried out a set of experiments to study the effect of interactions between miR-103/107 and Wnt3a on ER stress and apoptosis. Preadipocytes were treated with Wnt3a in the presence/absence of miR-103/107 mimics. Wnt3a had an inhibitory effect on miR-103/107 levels (**Fig. 5A**). It was found that Wnt3a reduced ER stress, with the mRNA levels of *GRP78, CHOP, ATF4,* and *ATF6* being decreased by approximately 40–65%, and the protein levels of GRP78 and CHOP being reduced to 50–70% (Fig. 5B, C). Additionally, the mRNA levels of *Bad, Bim,* and *Bax* and the protein levels of Bax and caspase-3 were also downregulated, while Bcl2 mRNA and protein level were increased (Fig.5D, E), indicating that Wnt3a inhibited apoptosis and ER stress. Also, Wnt3a was found to decrease caspase-3 activity to 63% compared with the control (Fig. 5G). TUNEL staining showed that Wnt3a treatment reduced the number of apoptotic cells (Fig. 5F). Flow cytometric analysis also indicated that Wnt3a reduced the number of apoptotic cells from 54.47 ± 5.22% to 39.68 ± 4.94% (Fig. 5H), which was similar to the results previously observed with miR-103/107 inhibitor. In addition, extra addition of miR-103/107 mimics reversed the repressive effects of Wnt3a on ER stress and apoptosis, as the levels of GRP78, CHOP, ATF4, ATF6, Bad, Bim, Bax, and caspase-3 were elevated, while the Bcl2 level was decreased compared
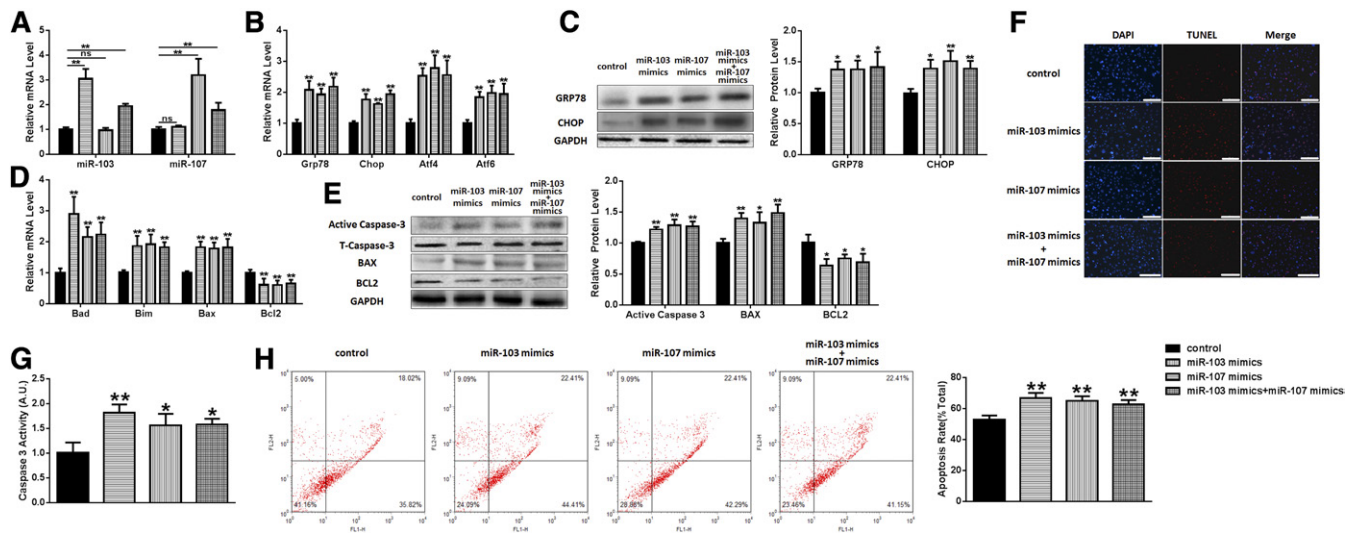
Fig. 3. Overexpressing miR-103/107 promoted preadipocyte ER stress and apoptosis. Preadipocytes were transfected with miR-103/107 mimics or control. A: The changes of miR-103 and -107. B: The changes of *GRP78*, *CHOP*, *ATF4*, and *ATF6* mRNA levels. C: The changes of GRP78 and CHOP protein levels. D: The changes of *Bad*, *Bim*, *Bax*, and *Bcl2* mRNA levels. E: The changes of Bax, Bcl2, and caspase-3 protein levels. F: TUNEL staining assessed the effects of miR-103/107 mimics on preadipocyte apoptosis. G: Caspase-3 activity was measured. H: Flow cytometry was used to analyze the effects of miR-103/107 mimics on preadipocyte apoptosis. Data represent the mean ± SD. Scale bars: 200 μm (*P < 0.05; **P < 0.01; n ≥ 3).

with the Wnt3a treatment group (Fig. 5A–E). On the other hand, the proportion of apoptotic cells was shown to increase in the Wnt3a and miR-103/107 mimics group compared to the Wnt3a individual treatment group (Fig. 5F, H), which was consistent with our previous results.

miR-103/107 promoted preadipocyte ER stress and apoptosis by inhibiting the canonical Wnt/β-catenin pathway

As a canonical Wnt ligand, Wnt3a is qualified for activating the canonical Wnt/β-catenin signaling pathway;

so we next investigated to determine whether this pathway was involved in mediating miR-103/107-induced ER stress and apoptosis. The expression of nucleus β-catenin was monitored. Compared with the control, Wnt3a increased the nucleus β-catenin level by 70%, and addition of miR-103/107 mimics reduced the β-catenin level in the nucleus (**Fig. 6A**). Similarly, p-β-catenin immunofluorescent staining showed that Wnt3a treatment decreased the β-catenin phosphorylation level and the addition of miR-103/107 mimics reversed this effect (Fig. 6B). Furthermore, DKK1, a specific inhibitor of the canonical
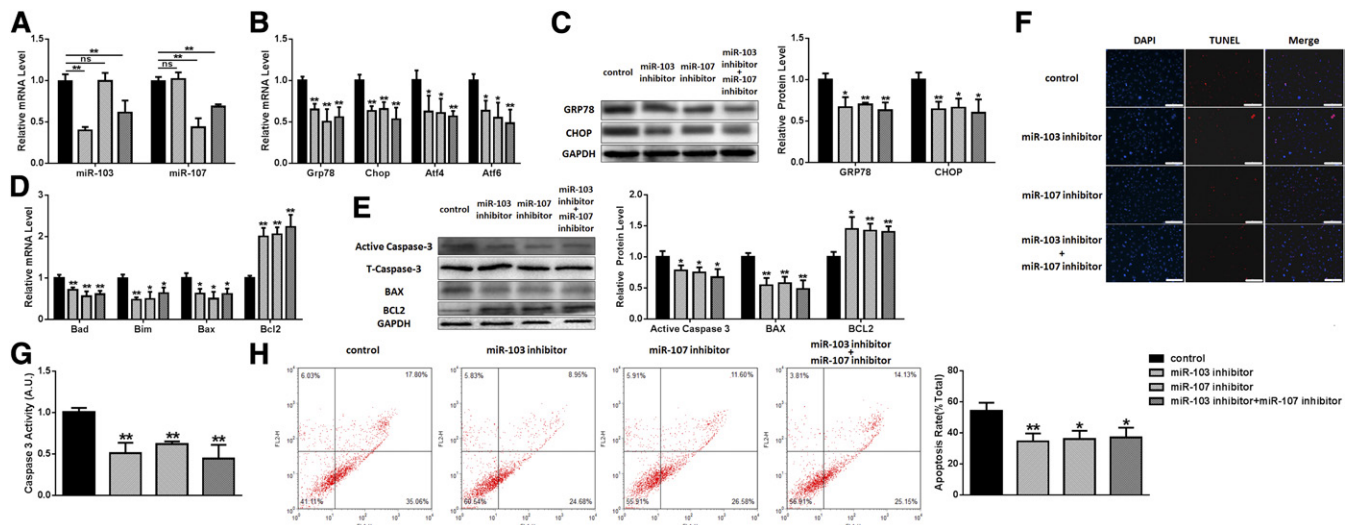

Fig. 4. Inhibition of miR-103/107 suppressed ER stress and apoptosis in preadipocytes. Preadipocytes were transfected with miR-103/107 inhibitor or control. A: The changes of miR-103 and -107. B: The changes of *GRP78*, *CHOP*, *ATF4*, and *ATF6* mRNA levels. C: The changes of GRP78 and CHOP protein levels. D: The changes of *Bad*, *Bim*, *Bax*, and *Bcl2* mRNA levels. E: The changes of Bax, Bcl2, and caspase-3 protein levels. F: TUNEL staining assessed the effects of miR-103/107 inhibitor on preadipocyte apoptosis. G: Caspase-3 activity was measured. H: Flow cytometry was used to analyze the effects of miR-103/107 inhibitor on preadipocyte apoptosis. Data represent the mean ± SD. Scale bars: 200 μm (*P < 0.05; **P < 0.01; n ≥ 3).
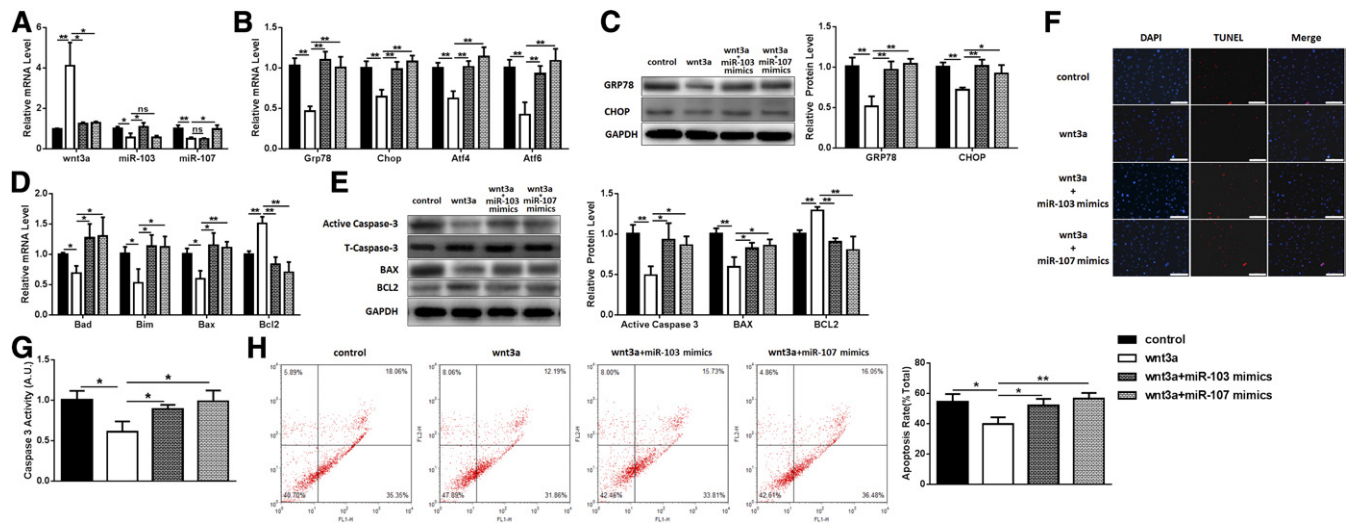
Fig. 5. Wnt3a relieved the effects of miR-103/107 on preadipocyte ER stress and apoptosis. Preadipocytes were transfected with Wnt3a vector with or without miR-103/107 mimics or control. A: The changes of Wnt3a, miR-103, and miR-107. B: The changes of *GRP78, CHOP, ATF4,* and *ATF6* mRNA levels. C: The changes of GRP78 and CHOP protein levels. D: The changes of *Bad, Bim, Bax,* and *Bcl2* mRNA levels. E: The changes of Bax, Bcl2, and caspase-3 protein levels. F: TUNEL staining assessed the effects of Wnt3a and miR-103/107 on preadipocyte apoptosis. G: Caspase-3 activity was measured. H: Flow cytometry was used to analyze the effects of Wnt3a and miR-103/107 on preadipocyte apoptosis. Data represent the mean ± SD. Scale bars: 200 μm (*$P < 0.05$; **$P < 0.01$; n ⩾ 3).

Wnt/β-catenin signaling pathway, was used for verification. We found that DKK1 raised the expression levels of GRP78, CHOP, caspase-3, and Bax by 39, 62, 73, and 38%, respectively, and the Bcl2 level was decreased by 36% (Fig. 6C), indicating that canonical Wnt/β-catenin signaling inhibition blocked miR-103/107-induced ER stress and apoptosis. Addition of Wnt3a relieved the effects of DKK1, and combination with miR-103/107 mimics reversed these effects again (Fig. 6C). These data suggested that miR-103/107 promoted preadipocyte ER stress and apoptosis by inhibiting the canonical Wnt/β-catenin pathway at least partially.

ATF6 is essential in miR-103/107-promoted ER stress and apoptosis

To clarify the mechanism of how miR-103/107 promoted ER stress, a series of bioinformatics analyses were conducted. We found two putative binding sites of LEF1, an important transcription factor downstream of the canonical Wnt/β-catenin signaling pathway, in the *ATF6* promoter region (from −1 to −2000). It had been found that activating canonical Wnt/β-catenin signaling by Wnt3a treatment resulted in a decreased *ATF6* mRNA level (Fig. 5B). To determine whether LEF1 is critical for the regulation of the *ATF6* promoter, two sites were mutated
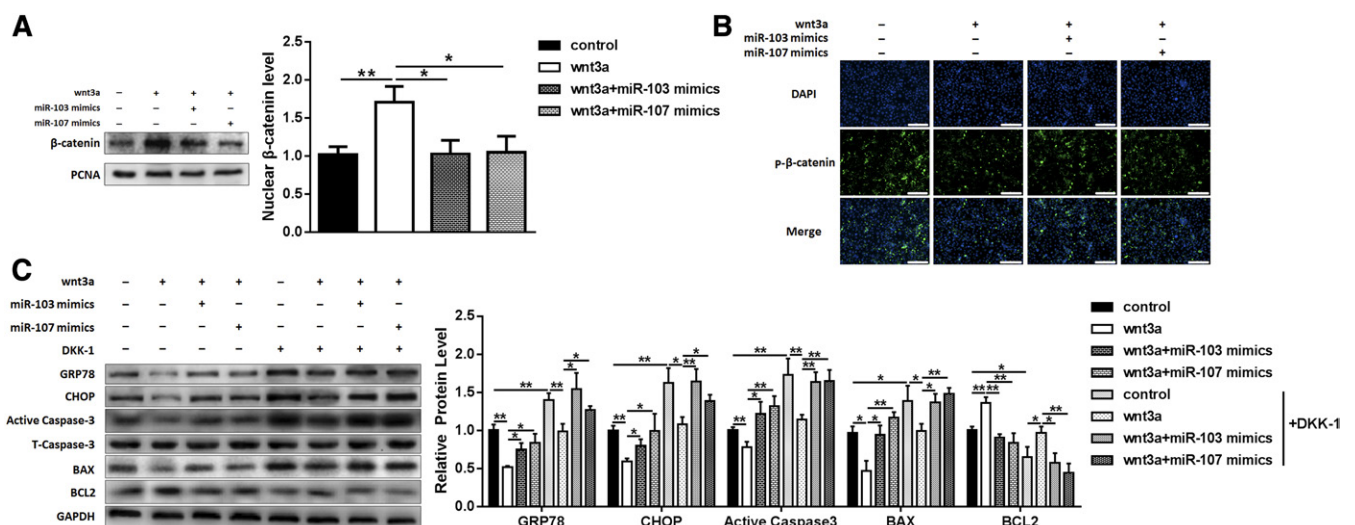

Fig. 6. miR-103/107 promoted preadipocyte ER stress and apoptosis by inhibiting the canonical Wnt/β-catenin pathway. Preadipocytes were treated with Wnt3a vector with or without miR-103/107 mimics or control, and DKK1 was added into medium 3 h before collection. A: The changes of nucleus β-catenin level. B: The p-β-catenin immunofluorescent staining. C: The changes of protein levels of GRP78, CHOP, Bax, Bcl2, and caspase-3. Data represent the mean ± SD. Scale bars: 200 μm (*$P < 0.05$; **$P < 0.01$; n ⩾ 3).
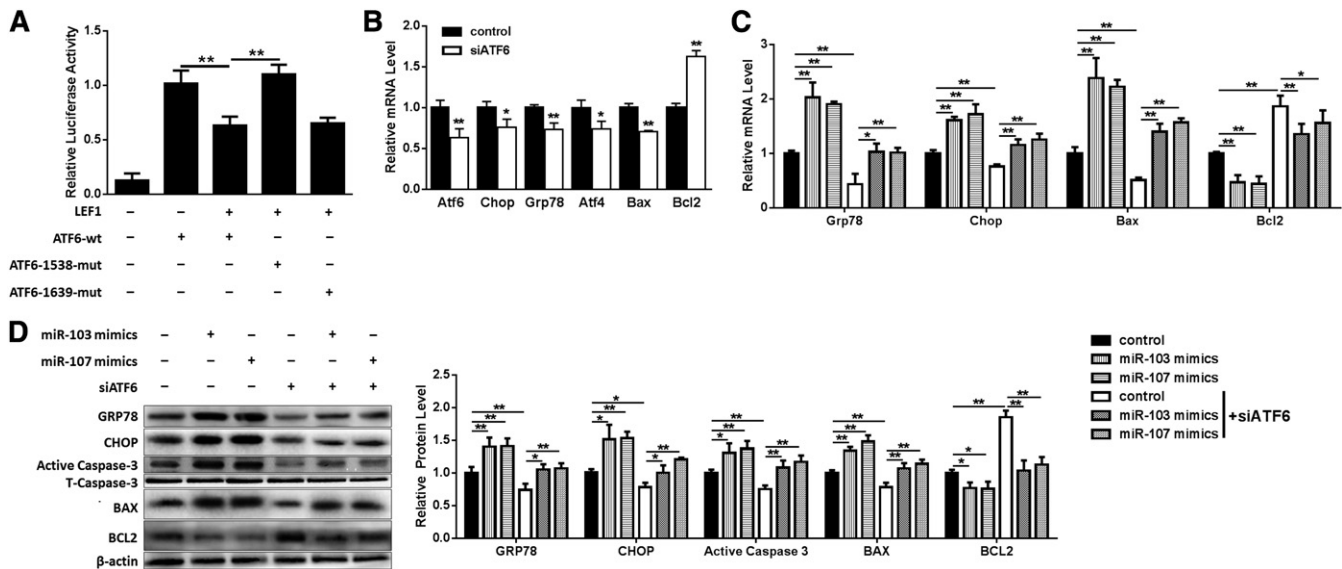
Fig. 7. ATF6 is essential in miR-103/107 promoted ER stress and apoptosis. A: Dual-luciferase reporter assays were performed to test *ATF6* promoter activity. B: qPCR was used to analyze the effects of siATF6 on *GRP78*, *CHOP*, *ATF4*, *Bax*, and *Bcl2*. Preadipocytes were treated with miR-103/107 mimics with or without siATF6 (C, D). C: qPCR was performed to detect the changes of *GRP78*, *CHOP*, *Bax*, and *Bcl2* mRNA levels. D: The protein levels of GRP78, CHOP, Bax, Bcl2, and caspase-3. Data represent the mean ± SD (*$P < 0.05$; **$P < 0.01$; n ≥ 3).

and *ATF6* promoter activity was determined. Overexpressing LEF1 resulted in a 36% decrease of *ATF6* promoter activity, and mutation of the −1538 binding site experienced a 73% increase in *ATF6* promoter activity compared with the wild-type group, while there was no difference between the mutation of the −1639 binding site group and the wild-type group (**Fig. 7A**), suggesting that the −1538 binding site is critical for LEF1 negative regulation of *ATF6*.

siATF6 was then used to silence ATF6 to determine whether ATF6 plays a key role in miR-103/107-promoted ER stress and apoptosis. It was found that siATF6 downregulated *ATF6*, *GRP78*, *CHOP*, *ATF4*, and *Bax* mRNA levels, and upregulated the *Bcl2* mRNA level (Fig. 7B). Furthermore, siATF6 was shown to raise the *Bcl2* mRNA level by 86% and decrease *GRP78*, *CHOP*, and *Bax* mRNA levels to 43, 75, and 51%, respectively, which were elevated by miR-103/107 mimics (Fig. 7C). Western blot analysis was consistent with the results of mRNA (Fig. 7D). These results suggested that ATF6 is essential in miR-103/107-promoted ER stress and apoptosis.

Preadipocyte apoptosis induced by miR-103/107 was mediated by ER stress

We next addressed whether apoptosis induced by miR-103/107 was related to ER stress; we used 4-PBA as an ER stress inhibitor to relieve ER stress. These results demonstrated that the expression levels of GRP78, CHOP, caspase-3, and Bax were significantly repressed and the Bcl2 expression level was enhanced in the 4-PBA-pretreated group (**Fig. 8A**). Compared with miR-103/107 mimics treatment, 4-PBA pretreatment rescued the levels of GRP78, CHOP, caspase-3, Bax, and Bcl2 (Fig. 8A).

In order to understand how ER stress mediated miR-103/107-induced apoptosis, bioinformatics analyses revealed that the *Bcl2* promoter region (from −1 to −2000) contained

a putative ATF6 binding site (−385). We found that overexpressing ATF6 inhibited the mRNA level of *Bcl2* (Fig. 8B). The role of ATF6 on *Bcl2* transcription was confirmed by dual-luciferase reporter assays. The wild-type of the binding site resulted in a 54% decrease in *Bcl2* promoter activity, and the mutation of the *Bcl2* promoter led to a 95% increase compared with the wild-type group (Fig. 8C), suggesting that ATF6 negatively regulates *Bcl2* transcription. It was also found that knockdown Bcl2 by siBcl2 had no effect on ER stress, as the mRNA levels of *ATF6*, *GRP78*, and *CHOP* remained unchanged (Fig. 8D). In contrast, the *Bax* mRNA level was increased to 153%, while the *Bcl2* mRNA level was decreased to 68% (Fig. 8D), suggesting that Bcl2 plays a role in apoptosis. We then determined the levels of ER stress and apoptosis after transfection of miR-103/107 mimics in the presence/absence of siBcl2. These studies revealed that siBcl2 had no effect on miR-103/107-activated ER stress (Fig. 8E). On the contrary, siBcl2 treatment upregulated Bax and caspase-3, and Bcl2 was downregulated (Fig. 8E). These results indicated that ER stress mediated miR-103/107-induced apoptosis and ATF6 was essential during this process.

DISCUSSION

With social development, the number of obese adolescents is on the rise. More seriously, obesity-related lifestyles and their health hazards will continue to adulthood, increasing the risk of obesity, high blood pressure, heart disease, and other chronic noncommunicable diseases (29, 30). Obesity has become one of the serious public health problems that endanger the health of children and adolescents. Except for exercise, there are two methods of treatment for obesity at this stage: drug treatment and bariatric surgery. However, drug treatment has too many unacceptable
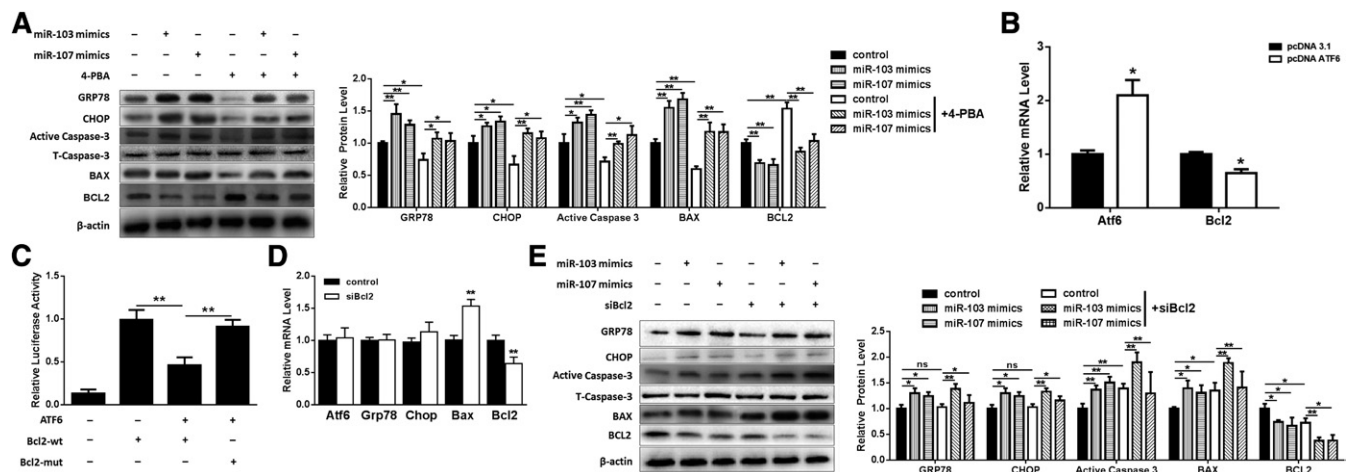
Fig. 8. miR-103/107-promoted preadipocyte apoptosis was mediated by ER stress. A: Preadipocytes were treated with miR-103/107 mimics with or without 4-PBA. Western blot was performed to detect the expression changes of GRP78, CHOP, Bax, Bcl2, and caspase-3. B: qPCR was used to detect the effect of ATF6 on *Bcl2*. C: Dual-luciferase reporter assays were performed to detect *Bcl2* promoter activity. D: The effect of siBcl2 on *ATF6*, *GRP78*, *CHOP*, *Bax*, and *Bcl2* mRNA levels. E: Preadipocytes were treated with miR-103/107 mimics with or without siBcl2. Western blot analyses were performed to detect the changes of GRP78, CHOP, Bax, Bcl2, and caspase-3. Data represent the mean ± SD (*$P < 0.05$; **$P < 0.01$; n ⩾ 3).

side effects and bariatric surgery is not suitable for all obese patients. Considering these problems, inducing apoptosis to reduce adipocyte number may be an effective approach for obesity treatment. Our previous studies have shown that regulation of apoptosis in adipose tissue has the potential to form the basis of a future treatment of obesity (31–35).

A great number of miRNAs have been implicated in the apoptosis process. For example, miR-125b resisted breast cancer cells via suppressing Bak expression (36). miR-187, miR-181c, and miR-34a also have been proven to regulate apoptosis and inflammation by directly targeting TNF-α (37–39). miR-103 and -107 are paralogs, which differ only at one nucleotide near their 3′ ends and reside on different human chromosomes. Their host genes are conserved in all known vertebrates (40).

It has been reported previously that miR-103/107 regulated adipose insulin sensitivity (12). In order to study the effect of miR-103/107 on preadipocytes, bioinformatics analyses were carried out to predict their target genes. We found that the 3′-UTR region of Wnt3a includes a potential binding site for miR-103/107 with a 7 nt match. Interestingly, a previous study in epithelial stem cells had shown that miR-103/107 increased the proliferative capacity of keratinocytes by targeting Wnt3a (41). We employed a dual-luciferase reporter system to confirm that miR-103/107 targets Wnt3a in preadipocytes.

As Wnt3a is a canonical Wnt ligand, we examined the β-catenin phosphorylation level and found that miR-103/107 blocked the canonical Wnt/β-catenin signaling pathway. Canonical Wnt/β-catenin signaling pathways are involved in a variety of cell activities, including apoptosis (42, 43). As a main ligand of Wnt/β-catenin signaling pathways, Wnt3a binds to the specific receptor, delivering the signal to β-catenin, which accumulates as an important substance in the nucleus and regulates the expression of the relevant target genes (15, 16). In the deficiency of Wnt ligands, the intracellular β-catenin is degraded by a polyprotein complex

consisting of Axin/APC/GSK3/DK1, resulting in a low level of β-catenin. In this study, we found that LEF1 regulated *ATF6* promoter activity, indicating that ATF6 is a target gene of the Wnt/β-catenin signaling pathway. In preadipocytes, miR-103/107 were shown to suppress Wnt3a expression, block Wnt/β-catenin signaling, and degrade β-catenin, resulting in releasing the inhibitory effect of LEF1 on ATF6 and the onset of activated ATF6-related ER stress (**Fig. 9**).

Apoptosis exists through the whole life process of multicellular organisms, which can remove the excess and damaged cells in the body in time and maintain the stability of tissues and organs. Apoptosis, as a mechanism of programmed cell death, is critical for cell homeostasis, which allows the deletion of redundant cells in a controlled manner (44). There are three apoptotic pathways in eukaryotic cells: the death receptor-mediated extrinsic pathway, the intrinsic mitochondrial pathway, and the ER stress-mediated pathway, which we studied in our research (45). When the intracellular environment changes, such as during hypoxia, hypoglycemia, and oxidative stress, unfolded proteins accumulate on the ER, thus resulting in unfolded protein response through the ER stress sensors located in the ER membrane: IRE1α, PERK, and ATF6. However, if ER stress continues at a high level, the adaptation mechanisms are useless, ER stress is irreparable, and the sensors produce signal transduction to promote apoptosis by modulating Bcl2 family proteins or regulating calcium channels on the ER (46). In this study, we have shown that ATF6 transcriptionally inhibited *Bcl2* promoter activity, thus firmly demonstrating a link between ER stress and apoptosis in preadipocytes.

This study has concentrated on the effect of miR-103/107 on preadipocyte apoptosis. Studies have shown that miR-103/107 is highly expressed in adipose tissue, and palmitate and serum-free medium treatment induced ER stress and apoptosis accompanied by upregulated miR-103/107 levels, suggesting that miR-103/107 may play
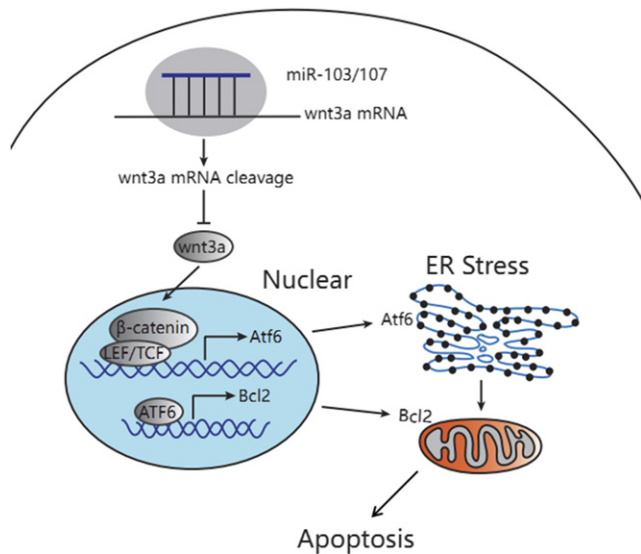
Fig. 9. miR-103/107 promoted ER stress-mediated apoptosis via the Wnt3a/β-catenin /ATF6 pathway in preadipocytes. miR-103/107 blocked wnt/β-catenin signaling by targeting Wnt3a, released the inhibitory effect of LEF1 on ATF6, and activated ATF6-related ER stress. On the other hand, ATF6 transcription inhibited Bcl2, finally inducing apoptosis.

important roles in the control of ER stress and apoptosis. We had demonstrated that overexpression of miR-103/107 by miR-103/107 mimics promoted ER stress and apoptosis, while knockdown of miR-103/107 by miR-103/107 inhibitor suppressed ER stress and apoptosis. Using bioinformatics and cellular and molecular biology methods, we confirmed that miR-103/107 targeted Wnt3a to promote ER stress and apoptosis in preadipocytes. Moreover, bioinformatics and luciferase assays indicated that ATF6 and Bcl2 are key players linking miR-103/107-induced ER stress to apoptosis in preadipocytes. *ATF6* is regulated by LEF1 and ATF6 binds to the *Bcl2* promoter to further regulate apoptosis.

In conclusion, we have demonstrated that miR-103/107 suppressed Wnt3a expression, blocked the Wnt/β-catenin signaling pathway, and degraded β-catenin, resulting in releasing the inhibitory effect of LEF1 on ATF6 and the onset of activated ATF6-related ER stress. Furthermore, ATF6 transcriptionally inhibited Bcl2 promoter activity, finally activating apoptosis (Fig. 9). We propose that this miR-103/107-induced apoptosis pathway may provide an important target for developing new therapies for the treatment of obesity and metabolic syndrome.

REFERENCES

1. Ng, M., T. Fleming, M. Robinson, B. Thomson, N. Graetz, C. Margono, E. C. Mullany, S. Biryukov, C. Abbafati, S. F. Abera, et al. 2014. Global, regional, and national prevalence of overweight and obesity in children and adults during 1980–2013: a systematic analysis for the Global Burden of Disease Study 2013. *Lancet.* **384:** 766–781.
2. Swinburn, B., W. Dietz, and S. Kleinert. 2015. A Lancet Commission on obesity. *Lancet.* **386:** 1716–1717.
3. Chen, L., D. J. Magliano, and P. Z. Zimmet. 2011. The worldwide epidemiology of type 2 diabetes mellitus–present and future perspectives. *Nat. Rev. Endocrinol.* **8:** 228–236.
4. Bartel, D. P. 2004. MicroRNAs: genomics, biogenesis, mechanism, and function. *Cell.* **116:** 281–297.
5. Rupaimoole, R., and F. J. Slack. 2017. MicroRNA therapeutics: towards a new era for the management of cancer and other diseases. *Nat. Rev. Drug Discov.* **16:** 203–222.
6. Arner, P., and A. Kulyte. 2015. MicroRNA regulatory networks in human adipose tissue and obesity. *Nat. Rev. Endocrinol.* **11:** 276–288.
7. Moore, K. J. 2013. microRNAs: small regulators with a big impact on lipid metabolism. *J. Lipid Res.* **54:** 1159–1160.
8. Kornfeld, J. W., C. Baitzel, A. C. Konner, H. T. Nicholls, M. C. Vogt, K. Herrmanns, L. Scheja, C. Haumaitre, A. M. Wolf, U. Knippschild, et al. 2013. Obesity-induced overexpression of miR-802 impairs glucose metabolism through silencing of Hnf1b. *Nature.* **494:** 111–115.
9. Meerson, A., M. Traurig, V. Ossowski, J. M. Fleming, M. Mullins, and L. J. Baier. 2013. Human adipose microRNA-221 is upregulated in obesity and affects fat metabolism downstream of leptin and TNF-α. *Diabetologia.* **56:** 1971–1979.
10. Hennessy, E. J., F. J. Sheedy, D. Santamaria, M. Barbacid, and L. A. O'Neill. 2011. Toll-like receptor-4 (TLR4) down-regulates microRNA-107, increasing macrophage adhesion via cyclin-dependent kinase 6. *J. Biol. Chem.* **286:** 25531–25539.
11. Li, M., Z. Liu, Z. Zhang, G. Liu, S. Sun, and C. Sun. 2015. miR-103 promotes 3T3–L1 cell adipogenesis through AKT/mTOR signal pathway with its target being MEF2D. *Biol. Chem.* **396:** 235–244.
12. Trajkovski, M., J. Hausser, J. Soutschek, B. Bhat, A. Akin, M. Zavolan, M. H. Heim, and M. Stoffel. 2011. MicroRNAs 103 and 107 regulate insulin sensitivity. *Nature.* **474:** 649–653.
13. Nusse, R., and H. Clevers. 2017. Wnt/beta-Catenin Signaling, Disease, and Emerging Therapeutic Modalities. *Cell.* **169:** 985–999.
14. Kahn, M. 2014. Can we safely target the WNT pathway? *Nat. Rev. Drug Discov.* **13:** 513–532.
15. Belinsky, G. S., B. Sreekumar, J. W. Andrejecsk, W. M. Saltzman, J. Gong, R. I. Herzog, S. Lin, V. Horsley, T. O. Carpenter, and C. Chung. 2016. Pigment epithelium-derived factor restoration increases bone mass and improves bone plasticity in a model of osteogenesis imperfecta type VI via Wnt3a blockade. *FASEB J.* **30:** 2837–2848.
16. Go, G. W., R. Srivastava, A. Hernandez-Ono, G. Gang, S. B. Smith, C. J. Booth, H. N. Ginsberg, and A. Mani. 2014. The combined hyperlipidemia caused by impaired Wnt-LRP6 signaling is reversed by Wnt3a rescue. *Cell Metab.* **19:** 209–220.
17. MacDonald, B. T., K. Tamai, and X. He. 2009. Wnt/beta-catenin signaling: components, mechanisms, and diseases. *Dev. Cell.* **17:** 9–26.
18. Takada, I., A. P. Kouzmenko, and S. Kato. 2009. Wnt and PPARgamma signaling in osteoblastogenesis and adipogenesis. *Nat. Rev. Rheumatol.* **5:** 442–447.
19. Phillips, B. T., and J. Kimble. 2009. A new look at TCF and beta-catenin through the lens of a divergent C. elegans Wnt pathway. *Dev. Cell.* **17:** 27–34.
20. Hetz, C. 2012. The unfolded protein response: controlling cell fate decisions under ER stress and beyond. *Nat. Rev. Mol. Cell Biol.* **13:** 89–102.
21. Ron, D., and P. Walter. 2007. Signal integration in the endoplasmic reticulum unfolded protein response. *Nat. Rev. Mol. Cell Biol.* **8:** 519–529.
22. Hetz, C., E. Chevet, and H. P. Harding. 2013. Targeting the unfolded protein response in disease. *Nat. Rev. Drug Discov.* **12:** 703–719.
23. Kim, I., W. Xu, and J. C. Reed. 2008. Cell death and endoplasmic reticulum stress: disease relevance and therapeutic opportunities. *Nat. Rev. Drug Discov.* **7:** 1013–1030.
24. Liu, Z., L. Gan, D. Luo, and C. Sun. 2017. Melatonin promotes circadian rhythm-induced proliferation through Clock/histone deacetylase 3/c-Myc interaction in mouse adipose tissue. *J. Pineal Res.* **62:** doi:10.1111/jpi.12383.
25. Liu, Z., L. Gan, Y. Xu, D. Luo, Q. Ren, S. Wu, and C. Sun. 2017. Melatonin alleviates inflammasome-induced pyroptosis through inhibiting NF-kappaB/GSDMD signal in mice adipose tissue. *J. Pineal Res.* **63:** doi:10.1111/jpi.12414.
26. Gan, L., Z. Liu, W. Cao, Z. Zhang, and C. Sun. 2015. FABP4 reversed the regulation of leptin on mitochondrial fatty acid oxidation in mice adipocytes. *Sci. Rep.* **5:** 13588.
27. Liu, G., M. Li, M. Saeed, Y. Xu, Q. Ren, and C. Sun. 2017. αMSH inhibits adipose inflammation via reducing FoxOs transcription and blocking Akt/JNK pathway in mice. *Oncotarget.* **8:** 47642–47654.
28. Gan, L., Z. Liu, D. Luo, Q. Ren, H. Wu, C. Li, and C. Sun. 2017. Reduced endoplasmic reticulum stress-Mediated autophagy is required for leptin alleviating inflammation in adipose Tissue. *Front. Immunol.* **8:** 1507.

29. Spalding, K. L., E. Arner, P. O. Westermark, S. Bernard, B. A. Buchholz, O. Bergmann, L. Blomqvist, J. Hoffstedt, E. Naslund, T. Britton, et al. 2008. Dynamics of fat cell turnover in humans. *Nature.* **453:** 783–787.

30. Della-Fera, M. A., H. Qian, and C. A. Baile. 2001. Adipocyte apoptosis in the regulation of body fat mass by leptin. *Diabetes Obes. Metab.* **3:** 299–310.

31. Liu, Z., L. Gan, T. Wu, F. Feng, D. Luo, H. Gu, S. Liu, and C. Sun. 2016. Adiponectin reduces ER stress-induced apoptosis through PPARα transcriptional regulation of ATF2 in mouse adipose. *Cell Death Dis.* **7:** e2487.

32. Feng, M., L. Tian, L. Gan, Z. Liu, and C. Sun. 2014. Mark4 promotes adipogenesis and triggers apoptosis in 3T3–L1 adipocytes by activating JNK1 and inhibiting p38MAPK pathways. *Biol. Cell.* **106:** 294–307.

33. Gan, L., Z. Liu, W. Jin, Z. Zhou, and C. Sun. 2015. Foxc2 enhances proliferation and inhibits apoptosis through activating Akt/ mTORC1 signaling pathway in mouse preadipocytes. *J. Lipid Res.* **56:** 1471–1480.

34. Cao, W., M. Li, T. Wu, F. Feng, T. Feng, Y. Xu, and C. Sun. 2017. αMSH prevents ROS-induced apoptosis by inhibiting Foxo1/ mTORC2 in mice adipose tissue. *Oncotarget.* **8:** 40872–40884.

35. Liu, Z., H. Gu, L. Gan, Y. Xu, F. Feng, M. Saeed, and C. Sun. 2017. Reducing Smad3/ATF4 was essential for Sirt1 inhibiting ER stress-induced apoptosis in mice brown adipose tissue. *Oncotarget.* **8:** 9267–9279.

36. Zhou, M., Z. Liu, Y. Zhao, Y. Ding, H. Liu, Y. Xi, W. Xiong, G. Li, J. Lu, O. Fodstad, et al. 2010. MicroRNA-125b confers the resistance of breast cancer cells to paclitaxel through suppression of pro-apoptotic Bcl-2 antagonist killer 1 (Bak1) expression. *J. Biol. Chem.* **285:** 21496–21507.

37. Zhang, L., L. Y. Dong, Y. J. Li, Z. Hong, and W. S. Wei. 2012. The microRNA miR-181c controls microglia-mediated neuronal apoptosis by suppressing tumor necrosis factor. *J. Neuroinflammation.* **9:** 211.

38. Rossato, M., G. Curtale, N. Tamassia, M. Castellucci, L. Mori, S. Gasperini, B. Mariotti, M. De Luca, M. Mirolo, M. A. Cassatella, et al. 2012. IL-10-induced microRNA-187 negatively regulates TNF-α, IL-6, and IL-12p40 production in TLR4-stimulated monocytes. *Proc. Natl. Acad. Sci. USA.* **109:** E3101–E3110.

39. Guennewig, B., M. Roos, A. M. Dogar, L. F. Gebert, J. A. Zagalak, V. Vongrad, K. J. Metzner, and J. Hall. 2014. Synthetic pre-microRNAs reveal dual-strand activity of miR-34a on TNF-α. *RNA.* **20:** 61–75.

40. Martello, G., A. Rosato, F. Ferrari, A. Manfrin, M. Cordenonsi, S. Dupont, E. Enzo, V. Guzzardo, M. Rondina, T. Spruce, et al. 2010. A microRNA targeting dicer for metastasis control. *Cell.* **141:** 1195–1207.

41. Peng, H., J. K. Park, J. Katsnelson, N. Kaplan, W. Yang, S. Getsios, and R. M. Lavker. 2015. microRNA-103/107 family regulates multiple epithelial stem cell characteristics. *Stem Cells.* **33:** 1642–1656.

42. Clevers, H., and R. Nusse. 2012. Wnt/beta-catenin signaling and disease. *Cell.* **149:** 1192–1205.

43. Johnson, M. L., and N. Rajamannan. 2006. Diseases of Wnt signaling. *Rev. Endocr. Metab. Disord.* **7:** 41–49.

44. Poon, I. K., C. D. Lucas, A. G. Rossi, and K. S. Ravichandran. 2014. Apoptotic cell clearance: basic biology and therapeutic potential. *Nat. Rev. Immunol.* **14:** 166–180.

45. Herold, C., H. O. Rennekampff, and S. Engeli. 2013. Apoptotic pathways in adipose tissue. *Apoptosis.* **18:** 911–916.

46. Yoshida, H., K. Haze, H. Yanagi, T. Yura, and K. Mori. 1998. Identification of the cis-acting endoplasmic reticulum stress response element responsible for transcriptional induction of mammalian glucose-regulated proteins. Involvement of basic leucine zipper transcription factors. *J. Biol. Chem.* **273:** 33741–33749.